Vol.4 No.3
Summer 1993

MULTIHADRON PRODUCTION FOR $e^+ e^-$ FOR $\sqrt{S}$ FROM 50 TO 61 GeV, C. M. ENERGIES AND COMPARISON WITH MULTIHADRON PRODUCTION IN HADRONIC INTERACTIONS

M. E. Zomorrodian

Physics Department, Saga University, Saga 840, Japan

Abstract

Average values of $< 1 - T >$ where T is the thrust are presented for $e^+ e^-$ AMY data and are compared with their values in hadronic interactions. As far as possible, similar analysis techniques have been employed in the two different interactions. Similar variation with E_{cm} is observed for this average in both data. The values of $< P_T >$ and $< P_L >$ relative to the thrust axis in $e^+ e^-$ are similar to those in hadronic interactions. The thrust distributions at the same energies for the two different data are in rather good agreement at the higher T values. At the lower T values, however, the $e^+ e^-$ distribution shows more enhancement than that for hadronic interactions. We discuss a possible explanation for all these features.

Introduction

A topic of major interest in high energy collisions is to understand the dressing up process by which the quarks from the fundamental interactions emerge as observed hadrons (the so-called hadronization process). In reference [1], it is pointed out that there are some overall similarities on the jet properties between the hadronic and the $e^+ e^-$ data below 17 GeV centre of mass energies. They concluded that it could be due to similarities between these reactions at the fundamental quark level, or to the dominance of hadronization at these energies.

We extend this analysis to the centre of mass energies up to 61 GeV. The main reason for doing this is to find more information about the dynamical features of $e^+ e^-$ and hardonic interactions. The best candidate at present for explaining these features is the quark parton model dressed by quantum chromodynamics (QCD).

Keywords: Thrust; Quark; Gluon; Hadronization

According to the theory in [2], there are dynamical differences between these two different processes. This leads us to suspect that different mechanisms may generate the final state hadrons in two cases, and that these differences may be reflected on the structure of final state hadrons at certain energies.

The hadronic events with large transverse momenta are of particular interest in our analysis (i. e. $P_T > 2.$ GeV/c for at least one track in each event), because they give us a better chance of detecting the basic properties of hard scattering phenomenon in hadronic interactions. It is hoped that these events will allow an unravelling of the inner structure of the hadrons and will teach us how the constituents interact [3].

An idealized description of such a situation is given in Figure 1 which shows that the simplest configuration of a

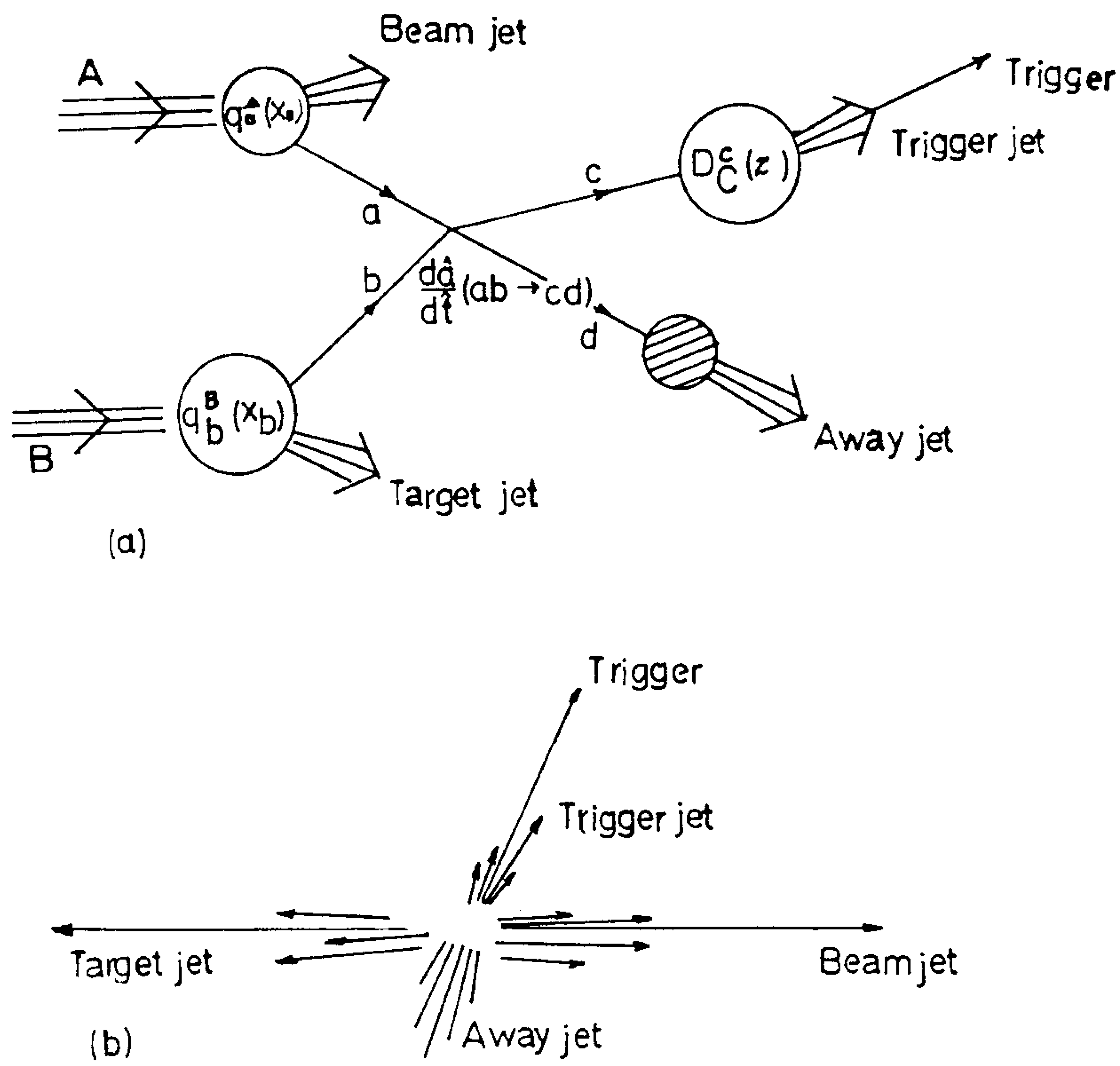

Figure 1. An idealized hard scattering process

large P_T hadron process implies the existence of at least four jets, two of which, the beam and the target jets, have long been familiar in multiparticle production physics and are of no interest to our analysis. A particle with high P_T, signals a possible jet and defines it as the 'toward jet' as opposed to 'away jet'.

The case of $e^+ e^-$ annihilation into hadrons at low energies is expected to proceed in essentially the same way (but without the presence of beam and target jets) and will thus be dominated by a two-jet structure arising from $\bar{q}\,q$ pair produced in the reaction $e^+ e^- \longrightarrow \bar{q}\,q$.

Figure 2 illustrates this situation. It shows that two back to back jets of hadrons sharing between them the momentum of the initial $\bar{q}$ or q and each having only a small momentum component transverse to the quark's direction of motions. It is also possible for one of the quarks to emit a "hard gluon" in which case there will be a three jet event as in Figure 3.

This paper is divided into four sections. In section 2 we describe the experimental procedure. In section 3 we present the comparison with hadron data. Section 4 summarizes our conclusions.

Experimental Procedure

The AMY detector, (Fig. 4) consists of a tracking detector and shower counter inside a 3-T solenoid magnetic coil which is surrounded by a steel flux return yoke followed by a muon detection system. The charged-particle tracking detector consists of a 4-layer cylindrical

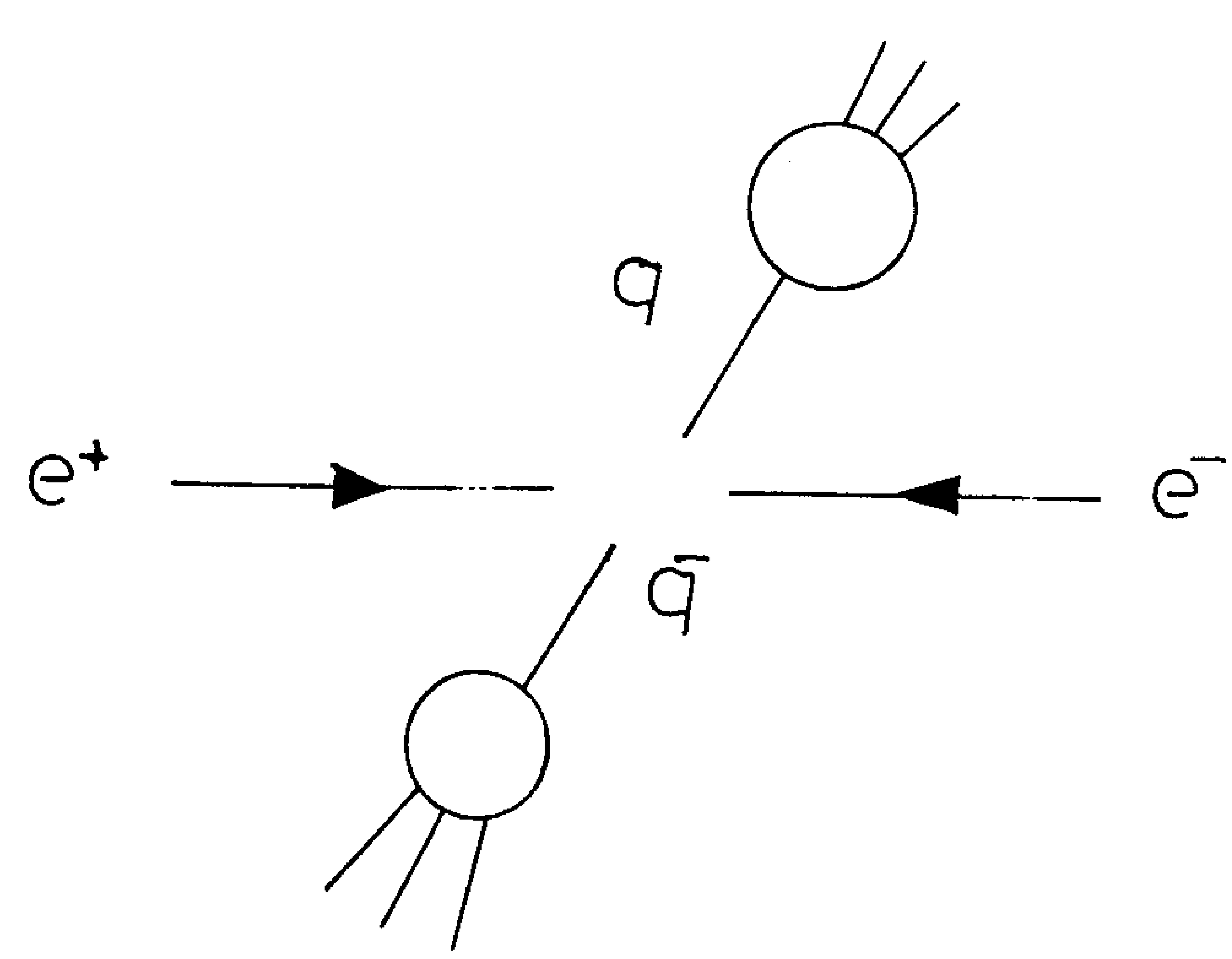

Figure 2. The process $e^+ e^- \longrightarrow 2$ jets

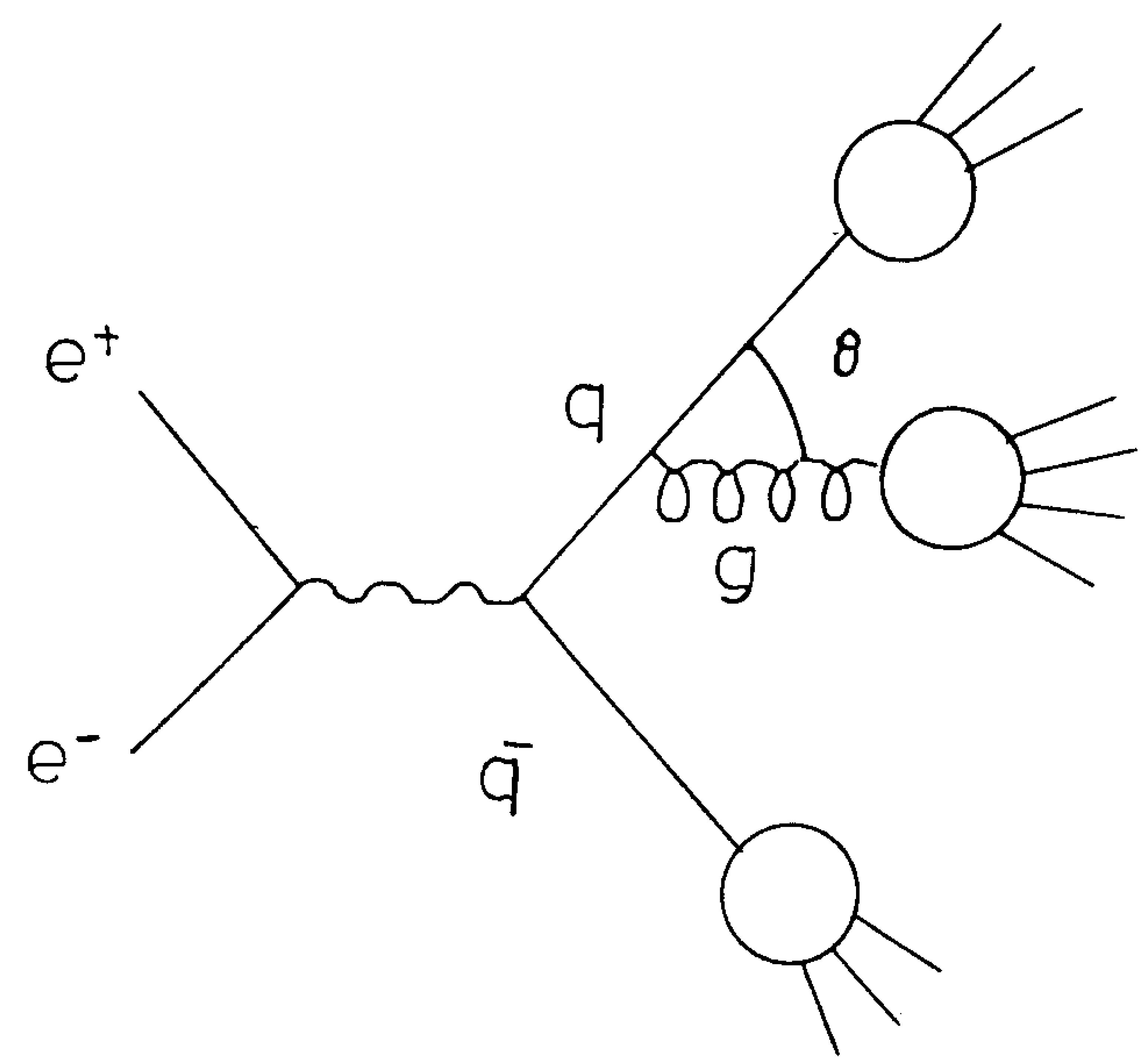

Figure 3. The process $e^+ e^-$ ——> 3 jets

array of drift tubes (inner tracking chamber, or ITC) and a 40-layer cylindrical drift chamber (central drift chamber, or CDC) with 25 axial layers of wires and 15 stereo layers. Charged particles are detected efficiently over the polar angle region $cos\theta < 0.87$ with a momentum resolution $\triangle PT/PT = 0.7\%$ x $[PT$ (GeV/c)]. Radially outside of the CDC is a 15-radiation-length cylindrical electromagnetic calorimeter (barrel shower counter, or SHC) which serves as a photon detector. The detector fully covers the angular region $cos\theta < 0.73$. Selection of multihadron final states from $e^+ e^-$ annihilation was based on the charged-particle momenta measured in the CDC and on the neutral-particle energy measured in SHC [4].

We have used a Monte Carlo program called PYTHIA for generating the hadronic events[1]. We have selected the hadronic events with at least one track with a $PT > 2.$ GeV/c. We have also removed the very slow momentum tracks say, $p < 0.35$ GeV/c from each event.

To investigate the jet properties of interactions, we

[1] We have generated data for both $\pi^- p$ and $p\,p$ interactions. This gave results which agreed within statistical errors with each other. So we refer to both as hadronic interactions.

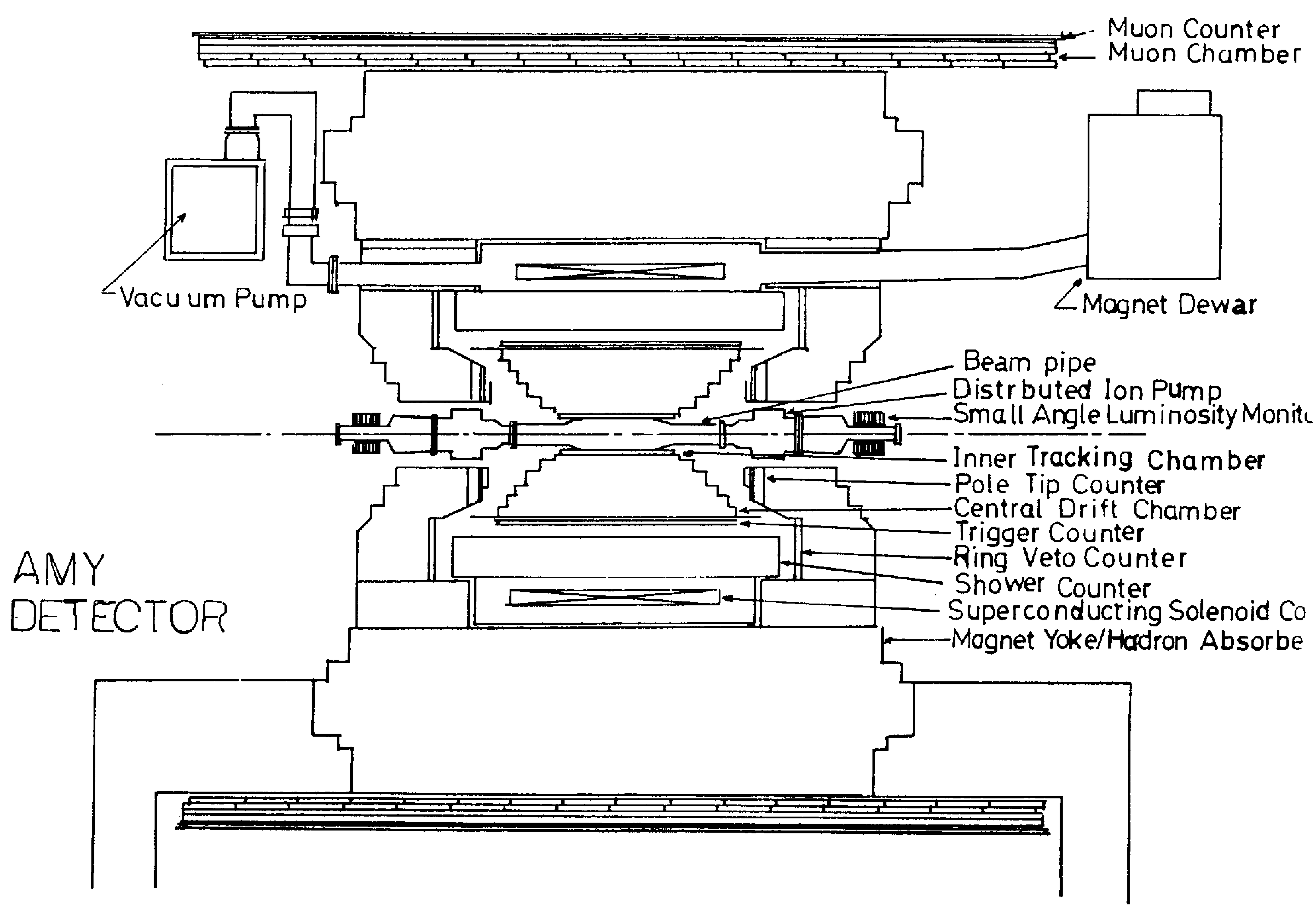

Figure 4. AMY Detector

look for an axis, such that the magnitudes of the particle's momentum component P_T transverse to that are minimized, while their longitudinal components, P_L, are maximized. One such measure is the variable thrust [5]:

$$T = \max \frac{\sum |P_{iL}|}{\sum |P_i|},$$

where the sum runs over all the particles in the event. If there are no jets and all momentum directions were equally probable, then $T = 1/2$. For perfect jets, all the hadrons would be travelling along a given axis so the extrema would be $T = 1$.

Comparison with Hadron Data

Figure 5 shows $< 1 - T >$ as a function of C.M. energies E_{cm} for $e^+ e^-$ and hadronic interactions. We have included the C. M. energies carried off by beam and target jets for the simulated hadronic interaction in our analysis, which is also the case for the low energy hadronic data [1]. The shape of the E_{cm} variation for $e^+ e^-$ below 20 GeV is similar to that for hadronic results. Furthermore, as the figure indicates, the values for simulated data are in good agreement with those for *AMY* data. $< 1 - T >$ do indeed become smaller by increasing the centre of mass energy. They do not vanish however, indicating that some hadrons have a finite P_T.

In part, this is presumably due to the confinement regime. In reference [6] it has been noted that partons which are confined within hadrons have a Fermi momentum component perpendicular to hadron's direction of motion, with $< k_t > \simeq 0.5$ GeV/c. And this is borne out by Figures 6 (a, b) where we show $<P_T>$ and $<P_L>$ relative to thrust axis separately for AMY data and for simulated hadronic data together with those obtained from other experiments at lower energies [1]. As the figure demonstrates, the values of $<P_T>$ and $<P_L>$ for simulated hadronic reactions appear to continue the same rising trend with energy as is seen in AMY results. Jet direction thus becomes better defined as the jet energy and hence the $<P_L>$ increases. However, it is seen that $<P_T>$ increases slowly with energy. This behaviour is also expected in QCD [7], because we must also consider diagrams such as Figure 3, for example, in which one of the quarks radiates a gluon.

To compare the $e^+ e^-$ and hadronic data in more detail, we show in Figure 7 the thrust distribution for AMY data at 60 GeV together with that for simulated hadronic data at the same energy. The AMY $e^+ e^-$ distribution with only two jet events is also plotted in the figure. As the figure illustrates, all distributions are in rather good agreement at high T. At low T, however, the distribution for the full AMY $e^+ e^-$ data shows more enhancement than that for hadronic data, and the distribution for hadronic data shows more contamination than that for the two jet $e^+ e^-$ events. This is probably due to the production of a high mass quark (i.e. bottom quark) which is more dominated in the case of AMY full data and is completely absent for the two jet $e^+ e^-$ events. This behaviour may also be interpreted as a radiation of a hard gluon from a quark which is probably again more dominated in the case of full $e^+ e^-$ annihilation data.

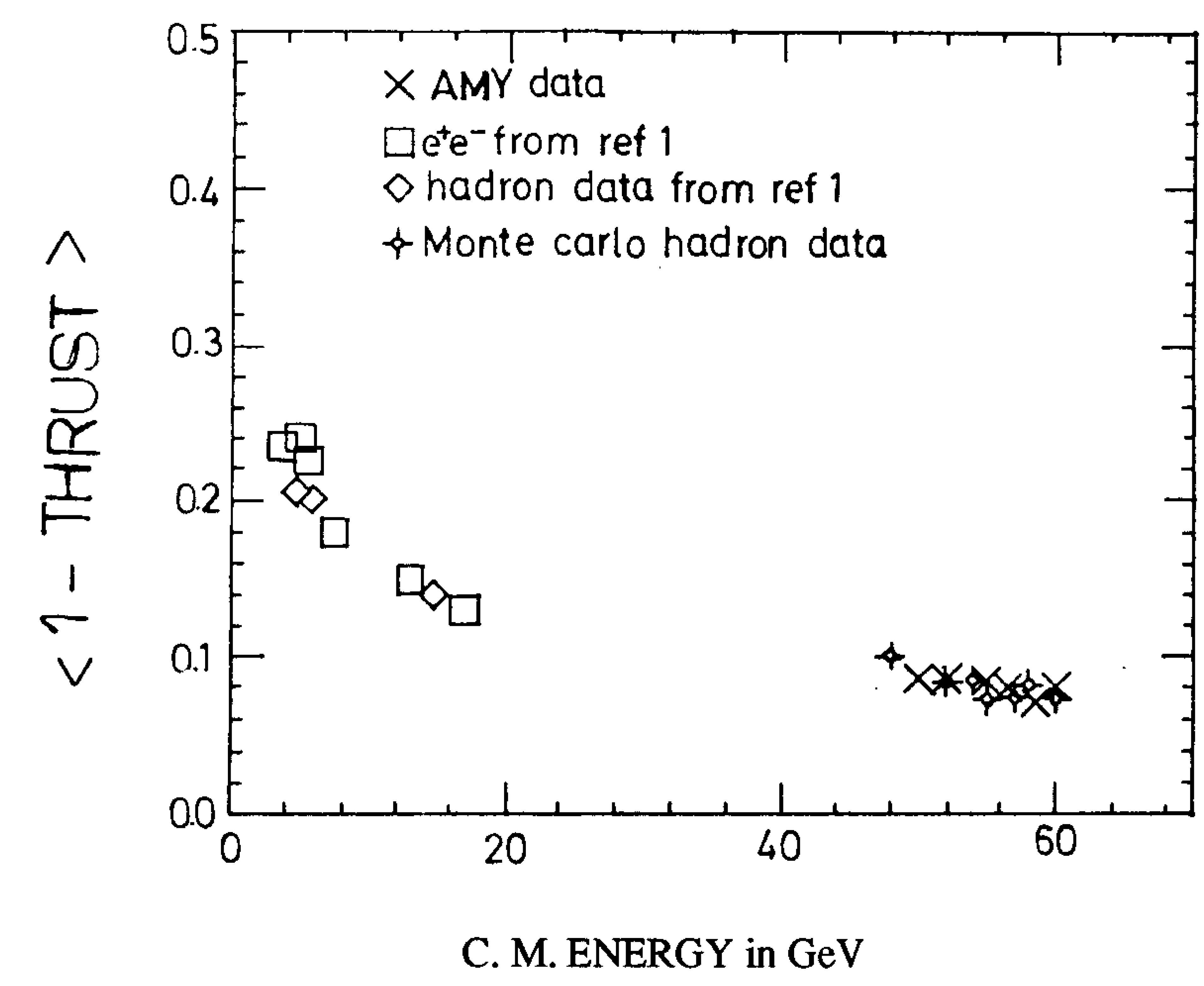

Figure 5. $< 1 - T >$ where T is the thrust for different reactions

It should be noted that in contrast to Figure 6, $e^+ e^-$ annihilation and hadronic simulation data are in good agreement in Figure 5. This means that <*PT*> and <*PL*> are insensitive to the thrust analysis.

Conclusion

We have calculated <1–*T*>, where *T* is thrust together with <*PT*> and <*PL*> relative to thrust axis for both AMY and simulated hadronic data. We observe the values of <1–*T*>, <*PT*> and <*PL*> for AMY data are in good agreement with the corresponding values for simulated hadronic results.

At 60 GeV centre of mass energy, the thrust distribution for both AMY and hadron data are in relatively good agreement at high *T*. However, AMY data shows more enhancement at lower *T* values. This is probably due to the fact that there is more possibility of a high mass quark production for the case of $e^+ e^-$ annihilations. This effect may also be due to a hard gluon emission from the $\bar{q}$ or q jet which is more dominant in $e^+ e^-$.

Generally, however, we observe an overall similarity between AMY and hadron data. We conclude that the jets

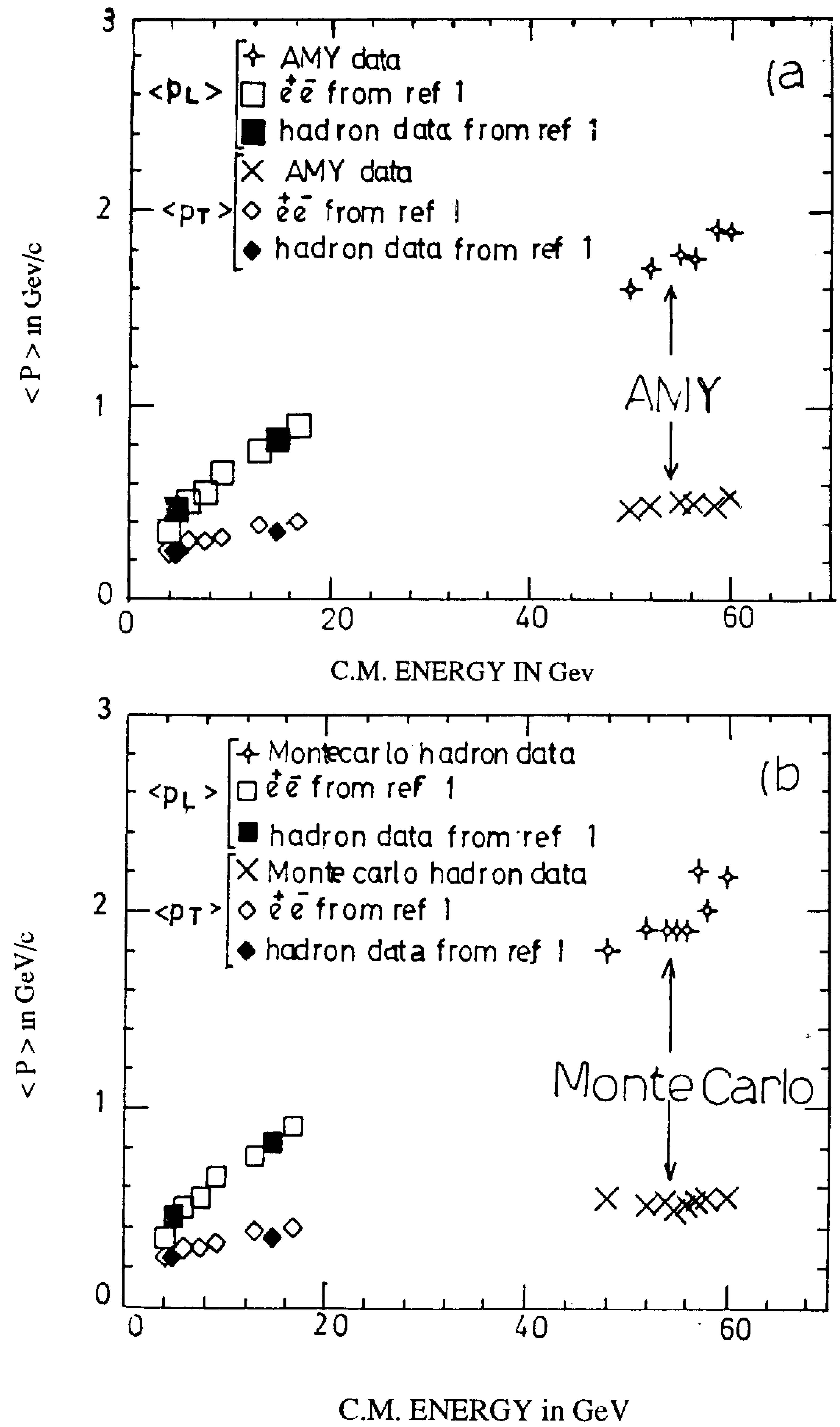

Figure 6. Average of *PL* and *PT* relative to thrust axis for both hadron data and $e^+ e^-$ data

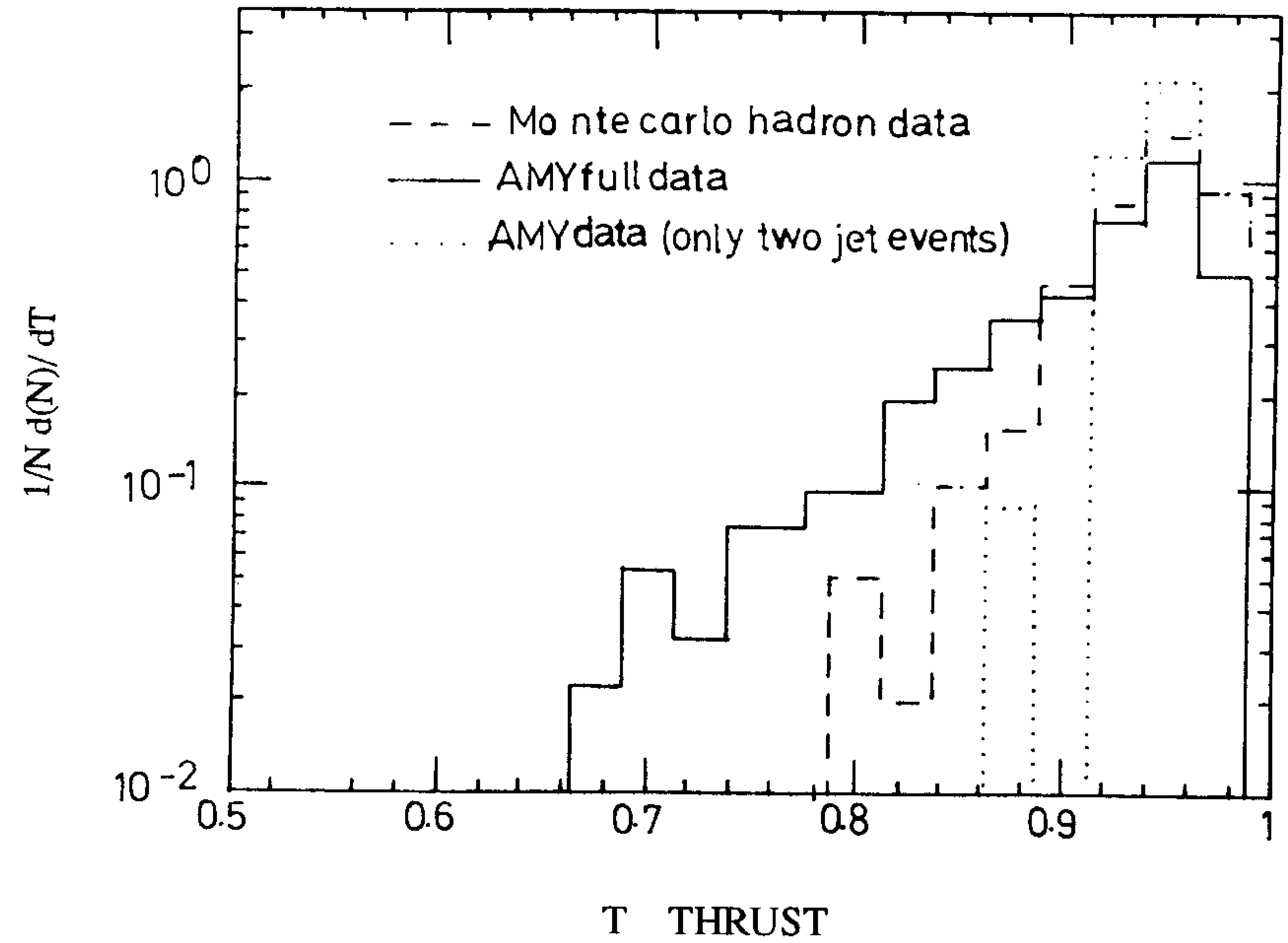

Figure 7. Thrust distribution relative to thrust axis for AMY data as well as for hadronic data at 60 GeV C. M. energy

seen in such different processes as hard scattering (Fig. 1) and $e^+ e^-$ ——> hadrons (Figs. 2,3) are quite clearly manifestations of the same underlying mechanism: the hadronization of fast-moving but confined partons [6]. The parton model dressed by QCD seems indispensable to the analysis of all these types of processes. This conclusion has also been established in ISR experiments [8,9], and also in jets at collider energies [10,11].

Acknowledgements

I would like to thank the KEK staff and the AMY Collaboration for giving me the opportunity of using the TRISTAN facilities and the AMY data for this analysis. I wish to thank Professor Itoh for giving me the chance to stay as visiting professor at Saga University. I am extremely grateful to Professor Kobayashi and Professor Murakami for stimulating discussions, for assistance, and for the careful reading of this manuscript. Thanks also to all the staff of Saga University for their very warm hospitality. The financial support given by the Islamic Republic of Iran is gratefully acknowledged.

References

1. Gottgens, R. *et al., Nucl. Phys.* **B178,** 392-400 (1981).
2. Ellis, J. *et al., Ibid.* **B111,** 253-271, (1976a). Berman, S. M., Bjorken, J. D. and Kogut, J. B. *Phys. Rev.* **D4,** 3388, (1971b), Preparate, G. *Nucl. Phys.* **B89,** 445 (1975c).
3. Jacob, M. and Landshoff, P. V. *Phys. Rep.* **48C,** 285, (1978).
4. AMY Collaboration, Li, Y. K. *et. al., Phys. Rev.* **D41,** 2675, (1990a). Kim, Y. K. *et al., Phys. Rev. Lett.* **63,** 1772 (1989b).
5. Brandt, S. and Dahmen, H. D. *Z. Phys.* **C1,** 61 (1979).
6. Hadron Interactions, Collins, P. D. B. and Martin, A. D., Adam Hilger Ltd., Bristol.
7. Naroska, B. DESY 86 - 113, (Sept. 1986).
8. Soding, P. Proceedings of the EPS Conference on High Energy Physics, CERN, Geneva, p. 271. (1979).
9. Jacob, M. *Ibid*, Geneva, p. 473, (1979).
10. UA1 Collaboration, Arnison, G. *et al., Phys. Lett.* **132B** 223, (1983a). *Ibid.* **123B,** 115, (1983b). *Ibid.* **132B,** 214, (1983c). *Ibid.* **129B,** 273, (1983d).
11. UA2 Collaboration, Bagnaia, P. *et al., Z. Phys.* **C20,** 117, (1983a), *Phys. Lett.* **122B,** 322, (1983b), *Ibid.* **129B,** 130 (1983c).